Macromolecules **1999,** *32,* 381−386

Characterization of the Molecular Environment of Polymer Langmuir−Blodgett Films Using a Pyrene Fluorescent Probe

Jun Matsui, Masaya Mitsuishi, and Tokuji Miyashita*

Institute for Chemical Reaction Science (ICRS), Tohoku University,
Katahira 2-1-1, Aoba, Sendai 980-8577, Japan

Received September 16, 1998; Revised Manuscript Received November 25, 1998

ABSTRACT: The molecular environment of polymer Langmuir−Blodgett (LB) films with different alkyl chain length, poly(*N*-dodecyl acrylamide) (pDDA) and poly(*tert*-pentyl acrylamide) (p*t*PA), which are copolymerized with a small amount of 1-pyrenylmethyl acrylate (PyMA) comonomer as a luminescent probe, was investigated by means of the surface pressure (π)−area (A) isotherms, UV−vis spectroscopy, and fluorescence spectroscopy. The pyrene ring orients perpendicular to the p(DDA/PyMA) layer in both the monolayer at the air/water interface and LB multilayers, while the pyrene moiety of p(*t*PA/PyMA) takes a parallel orientation to its layer plane. The pyrene residue is more exposed to its surroundings in p(*t*PA/PyMA) LB films and therefore sensitive to solvent polarity. The measurement of fluorescence anisotropy confirmed that the pyrene was densely packed in the LB films. These findings suggest that the molecular orientation of luminescent molecules can be controlled when the length of side chains is changed by only several angstroms in a polymer LB assembly system.

Introduction

The recent technical development for constructing ultrathin film assemblies by the Langmuir−Blodgett (LB) technique, the self-assembly (SA) method, and layer by layer deposition[1,2] provides fascinating possibilities of molecular design. Although the LB technique seems to be most complicated, it would be advantageous if we could arrange two-dimensional molecular assemblies in a specific planned order.[3]

Several researchers have attempted to provide photonic functionality with LB molecular assemblies. For example, Kuhn and co-workers have extensively investigated photophysical processes in LB films.[3] Patterson et al. demonstrated effects of molecular organization at the air−lipid boundary in a floating monolayer using a pyrene probe.[4,5] Yamazaki et al. reported on spectroscopic properties of pyrene-labeled fatty acid LB films using picosecond time-resolved fluorescence spectroscopy.[6,7] Ito and Tsujii et al. discussed photophysical processes of pyrene chromophores in polymer LB systems.[8,9] The distribution of the chromophore is obviously different in low molecular weight and polymer LB systems. The luminophore moieties can be distributed uniformly in a polymer monolayer, while they tend to form aggregates or crystals in a low molecular weight monolayer.

It is known that the long alkyl side chains are not necessarily essential to form a stable monolayer. In these observations, however, the polymer backbones should interact in some other manner, e.g., by hydrogen bonding and van der Waals forces, to support a close-packed two-dimensional network formation. In studies of a series of poly(alkyl acrylamide) LB films,[10−13] fairly short side chains, e.g., *tert*-pentyl[12] and adamantyl[13] acrylamide groups, could be examples of good candidates for forming stable polymer LB films. This implies that the surface and/or interface properties of these LB films are expected to be quite different from those of the conventional LB films which consist of polymers with long alkyl side chains.

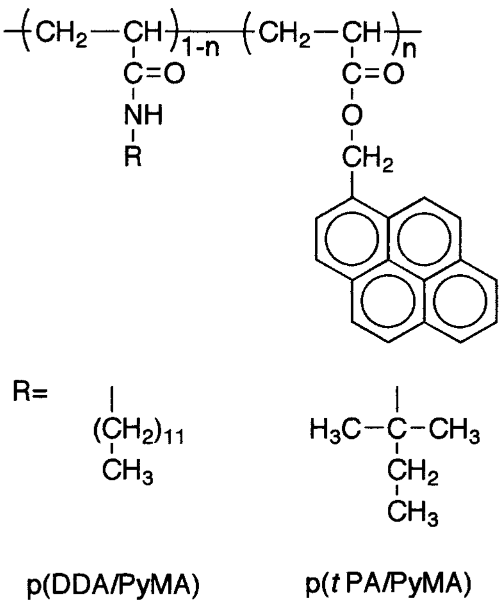

Figure 1. Molecular structure of p(DDA/PyMA)s and p(*t*PA/PyMA)s.

Considering these facts, we prepared two types of polymer LB films labeled with a luminescent pyrene probe (Figure 1): one with long alkyl and the other with short branched alkyl side chains. These LB films are interesting due to not only their fundamental properties[14] but also their applicational potential such as luminescent sensing materials. In the current study, we report on the molecular environment of these LB assemblies by means of the surface pressure (π)−area (A) isotherms, UV−vis spectroscopy, and fluorescence spectroscopy.

Experimental Section

1-Pyrenylmethyl acrylate monomer (PyMA) was synthesized by a similar procedure described elsewhere.[15] The copolymers

---

* To whom correspondence should be addressed. E-mail miya@icrs.tohoku.ac.jp.

10.1021/ma981471x CCC: $18.00

Table 1. Characterization of p(DDA/PyMA)s and p(*t*PA/PyMA)s Copolymers

	PyMA (mol %)	$M_w \times 10^{-4}$	M_w/M_n	area for PyMA (nm^2/unit)
p(DDA/PyMA3)	2.6	1.90	1.55	0.20
p(DDA/PyMA5)	5.0	3.71	1.47	0.22
p(DDA/PyMA9)	9.4	5.69	1.63	0.25
p(DDA/PyMA19)	18.8	6.44	1.52	0.067
p(*t*PA/PyMA1)	1.1	2.85	2.83	0.73
p(*t*PA/PyMA3)	2.8	7.08	1.40	0.99
p(*t*PA/PyMA10)	10.2	5.00	1.61	0.63

of PyMA with *N*-dodecylacrylamide (DDA) and with *tert*-pentylacrylamide (*t*PA) were prepared by free radical polymerization initiated by azoisobutylonitrile (AIBN) in toluene at 60 °C. The mole fraction of the pyrene chromophores in the copolymers was determined with UV−vis spectroscopy, using molar extinction coefficient for 1-pyrenylmethyl acrylate ($\epsilon = 4.6 \times 10^4$ M^{-1} cm^{-1}) at 345 nm in chloroform as reference. The molecular weights were determined by gel permeation chromatography using a polystyrene standard. They are summarized in Table 1. The measurement of $\pi-A$ isotherms and the deposition of monolayers were carried out with an automatic Langmuir trough (USI, LB lift Controller FSD-51 using a Wilhelmy-type film balance). Stable monolayers were prepared on the Langmuir trough (150 × 515 mm^2) in pure water (>17 MΩ·cm, Millipore Milli-QII) by spreading a 1×10^{-3} M chloroform solution at 15 °C and compressed at a rate of 15 cm^2/min. Quartz slides on which LB multilayers were deposited were cleaned in boiling HNO_3 solution and made hydrophobic by immersing the substrates in ca. 1×10^{-6} M octadecyltrichlorosilane (Tokyo Chemical Industry) solution in chloroform. The monolayers were transferred onto the substrates at a surface pressure of 25 mN/m with a dipping speed of 10 mm/min (up) and 5 mm/min (down). The transfer ratio was almost unity through the dipping process. Cast films were prepared from a 1×10^{-3} M chloroform solution of the copolymer. Fluorescence spectra and UV−vis absorption spectra were measured with a Hitachi F-4500 spectrofluorophotometer and a Hitachi U-3000 UV−vis spectrophotometer, respectively.

Results and Discussion

Monolayer Formation. The copolymers containing 1.0−20 mol % of the pyrene label were prepared, and their $\pi-A$ isotherms were measured (Figure 2a,b). All of the pDDA copolymers showed a steep rise in surface pressures and fairly high collapse pressures. This means that the copolymer monolayers are densely packed at the air/water interface. Here the averaged limiting surface area was estimated by extrapolating the linear portion of the condensed state in the $\pi-A$ isotherms to zero surface pressure. Using this value, the limiting surface area of the pyrene monomer unit was calculated assuming that the area for a DDA unit is 0.28 nm^2/unit. As listed in Table 1, the molecular areas for PyMA from 2.6 to 9.4 mol % were almost the same; however, the PyMA area in p(DDA/PyMA19) was much smaller than that for other copolymers. As the contents of PyMA increase, it is likely that the monolayer could be unstable even though the collapse pressure was still high.

Figure 2b shows the $\pi-A$ isotherms for a series of p*t*PA. Although the collapse pressures were lower than those for p(DDA/PyMA)s, the surface pressures for p(*t*PA/PyMA)s also increased sharply. As described in a previous paper,[12] a closely packed monolayer arrangement is also achieved in p(*t*PA/PyMA)s. Furthermore, we observed no change in the area of both p(DDA/PyMA)s and p(tPA/PyMA)s on keeping the pressure at 25 mN/m. This means that the copolymers form a stable monolayer without any structural relaxation at the deposition pressure.

The limiting surface area of the pyrene unit for each p(*t*PA/PyMA) in Table 1 indicates that the area was about 3 times larger than that for p(DDA/PyMA)s.[16] A comparison of these results with the calculated values based on the CPK model shown in the bottom of Figure 2 suggests that the pyrene units of p(*t*PA/PyMA)s take a parallel orientation to the monolayer plane at the air/water interface, while they orient vertically to the water surface in the case of p(DDA/PyMA)s.

Fluorescence of p(DDA/PyMA)s and p(*t*PA/PyMA)s in Solution. Figure 3 shows the fluorescence emission spectra for (a) p(DDA/PyMA)s and (b) p(*t*PA/PyMA)s in tetrahydrofuran solution. The excitation wavelength was 310 nm, and the solution was degassed with argon flow for at least 15 min before the measurements. The molecular concentrations of the solutions were kept below 4×10^{-6} M. As shown in Figure 3, the fluorescence spectra of both p(DDA/PyMA)s and p(*t*PA/PyMA)s show the monomer (from 370 to 400 nm) and excimer emission bands (480 nm).[17] The excimer emission could be attributed to an intramolecular excimer formation in a single polymer chain, judging from the molecular concentration.[18] As the mole fraction of pyrene increases, the ratio of the excimer and monomer emission (I_E/I_M) is enhanced. Furthermore, the excitation spectra for p(DDA/PyMA)s with less than 10% pyrene content showed no change in peak position, although the peak position for p(DDA/PyMA19) shifted to longer wavelength (not shown here). The pyrene units seem to be distributed uniformly below 10.2 mol % of the pyrene-containing comonomer.

The I_E/I_M values are shown in Figure 4. The filled circles (●) were obtained for the copolymers of DDA with 1-pyrenyl acrylamide (PyAm), which has been reported previously.[19] This figure proves that the excimer formation depends on the length of the side chain and the flexibility of pyrene moieties; as the side chains are shortened, the pyrene residues become more accessible to each other. The pyrene moieties of p(DDA/PyAm)s are bound to the polymer backbone tightly, and this is why the I_E/I_M for p(DDA/PyAm)s are much smaller than those for copolymers of PyMA.

Molecular Orientation of Pyrene Molecules in Polymer LB Films. As shown in Figure 5a, the pyrene has two electronic transition moments;[20] the moment for the first band (A_{277}, $\lambda = 277$ nm) is known to be perpendicular to the molecular long axis, and the second band (A_{345}, $\lambda = 345$ nm) has a transition moment parallel to it. These transition moments lie in the plane of the chromophore. Thus, we can evaluate the orientation of the pyrene molecules from the ratio of the two absorption bands. Figure 5b,c shows the absorption spectra for p(DDA/PyMA3) and p(*t*PA/PyMA1) LB films with 40 layers. For a clearer view, each spectrum was normalized at wavelength $\lambda = 345$ nm. Since the absorption ratio A_{277}/A_{345} for p(DDA/PyMA3) is larger than that for p(*t*PA/PyMA1), the pyrene molecules must orient perpendicular to the layer plane in p(DDA/PyMA3) LB films, whereas they orient parallel to it in p(*t*PA/PyMA1) LB multilayers. The results are consistent with the discussion of the $\pi-A$ isotherms, which show smaller surface area for the pyrene chromophore in p(DDA/PyMA)s due to the perpendicular orientation

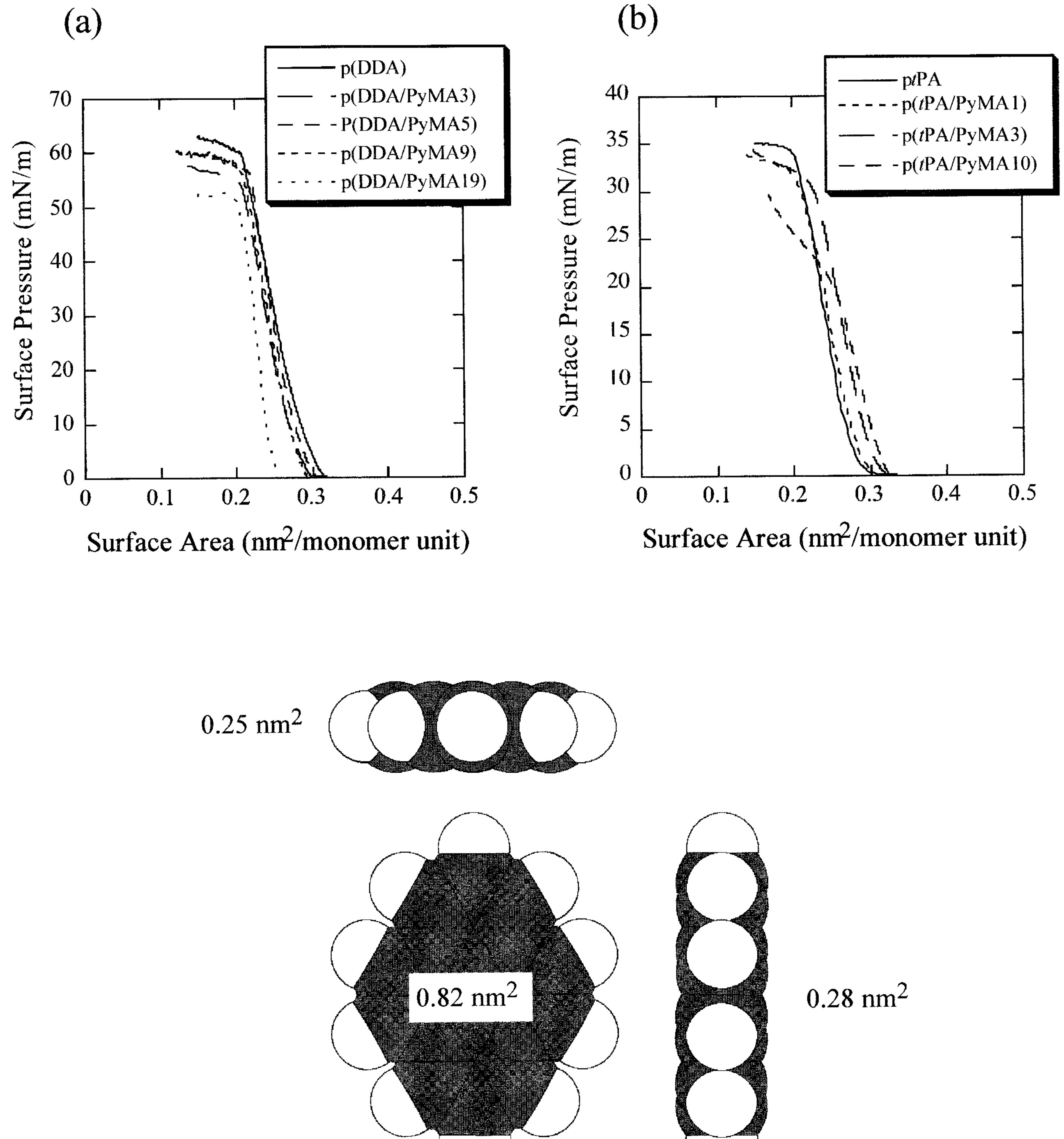

Figure 2. π–A isotherms for (a) p(DDA/PyMA)s and (b) p(tPA/PyMA)s at 15.0 °C (top) and the calculated area of cross section of a pyrene residue (bottom).

of the pyrene; i.e., the orientation of the pyrene is kept in both monolayers at the air/water interface and its multilayered films.

Molecular Environment of p(DDA/PyMA3) and p(*t*PA/PyMA1) in LB Films. It is well-known that the monomer fluorescence of pyrene is very sensitive to its surroundings,[21] i.e., the Ham effect. This effect is also expected in our case. As shown in Figure 3, the first emission band (I_1) observed at 379 nm is a symmetry-forbidden band, which is sensitive to the nature of the medium. When the pyrene molecule is surrounded by polar solvents, its symmetry can be broken due to the perturbation of vibronic coupling.[21] This leads to the enhancement of the emission intensity I_1, compared with that of other bands. The ratio of the emission intensity I_1 to that of the third band I_3 observed at 398 nm (I_1/I_3) has been often utilized to characterize the medium.[22,23] To investigate the molecular environment, it is preferable to minimize excimer emission, because it affects the third band at around 398 nm as shown in Figure 3. Thus, hereafter were used p(DDA/PyMA3) and p(tPA/PyMA1) with low pyrene contents. At first we measured the fluorescence spectra for these two copolymers in four solutions with different polarities. The results are listed in Table 2. The emission ratio I_1/I_3 increased, as expected with the solvent polarity, al-

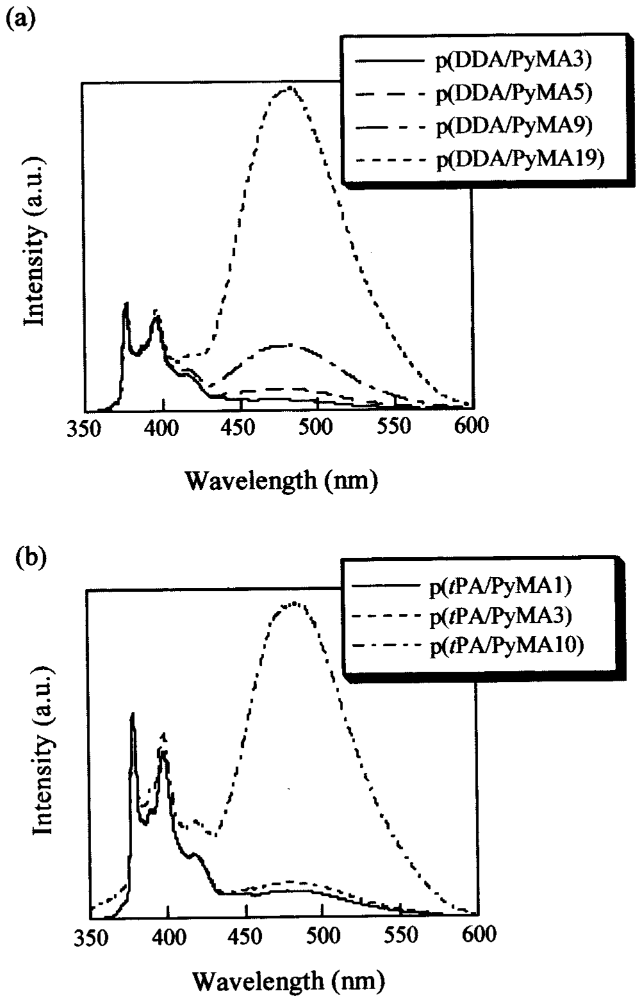

Figure 3. Fluorescence emission spectra for (a) p(DDA/PyMA)s and (b) p(*t*PA/PyMA)s in tetrahydrofuran. The pyrene residue's concentrations were kept below 4×10^{-6} M.

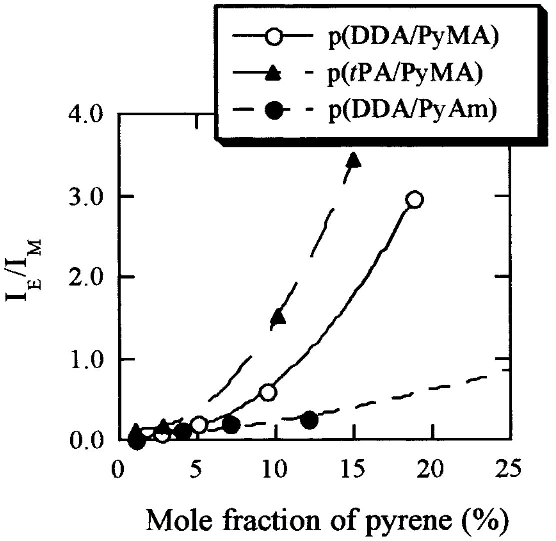

Figure 4. Dependence of I_E/I_M on mole fraction of PyMA in copolymer: (○) p(DDA/PyMA)s, (▲) p(*t*PA/PyMA)s, and (●) p(DDA/PyAm)s.

though less sensitive to solvent polarity than pyrene solutions.[22,23] When symmetry features of pyrene are broken by substituting a polar group for a hydrogen (in this case methyl acrylate), the ratio of I_1/I_3 would increase even in nonpolar solution.

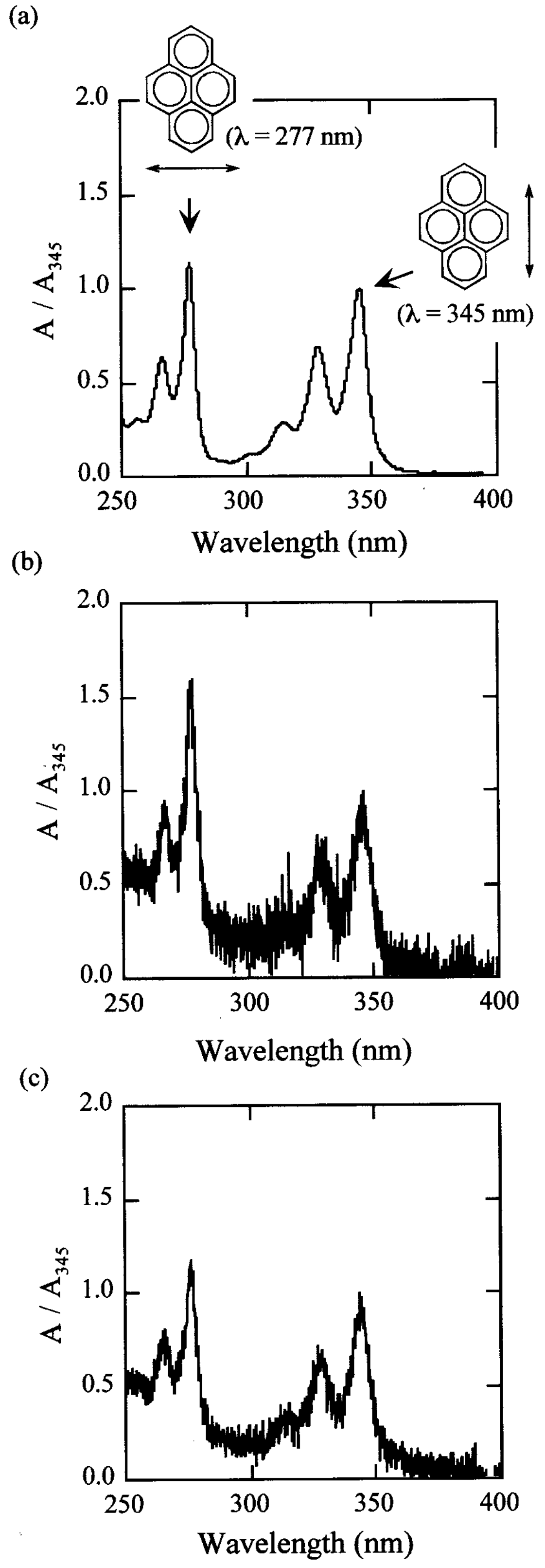

Figure 5. Absorption spectra for (a) p(DDA/PyMA3) in chloroform and (b) LB films of p(DDA/PyMA3) and (c) p(*t*PA/PyMA1) with 40 layers.

We employed LB films with the structure shown in the inset of Figure 6. Non-pyrene-labeled polymer LB films (pDDA 4 layers) were deposited in order to prevent substrate quenching, and then two layers of the pyrene-labeled copolymers were deposited. Figure 6 shows the fluorescence spectra for p(*t*PA/PyMA1) LB films in two

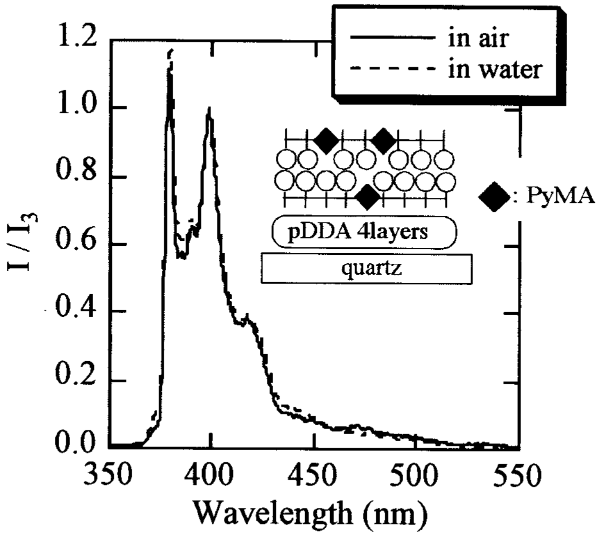

Figure 6. Fluorescence emission spectra of p(*t*PA/PyMA1) LB films in air (solid line) and in water (dashed line). Inset: the structure of the LB films used in the current study.

Table 2. Solvent Dependence of Fluorescence Emission Intensity I_1/I_3 Ratios of p(DDA/PyMA3) and p(*t*PA/PyMA1)

	I_1/I_3			
	tetrahydrofuran	ethanol	hexanol	cyclohexane
p(DDA/PyMA3)	1.18	1.15	1.13	1.07
p(*t*PA/PyMA1)	1.23	1.23	1.15	1.15

different surroundings: air and water. The emission ratio I_1/I_3 was 1.12 in air and 1.18 in water. On the other hand, the ratio was not changed for p(DDA/PyMA3) LB films (I_1/I_3 = 1.06). From the X-ray diffraction measurements, the thickness of each monolayer was determined as 1.0 nm (p*t*PA) and 1.8 nm (pDDA). Thus, the pyrene molecules are surrounded by dodecyl side chains in p(DDA/PyMA) LB films, while they were exposed to their surroundings at the p(*t*PA/PyMA) surface. Thus, the water molecules are more accessible to the pyrene units in p(*t*PA/PyMA1) LB than in p(DDA/PyMA3) LB films, leading to different I_1/I_3 ratios. It is also of interest that the excimer emission was constrained in LB films compared with that in solution (see Figures 3 and 6), suggesting that the molecular motion of the pyrene probe is restricted in LB films. We tried to evaluate in the following section the molecular motion of the pyrene in two different LB films.

Fluorescence Anisotropy in LB Films. The molecular motion of the pyrene residues in LB films was characterized by fluorescence depolarization. Fluorescence depolarization reflects the molecular motion when other factors, e.g., energy transfer, are negligible in the observed system. Polarizers were placed in front of both a light source (polarizer) and photodiode (analyzer). The ratio of fluorescence anisotropy *r* is obtained by changing the plane of the analyzer from parallel ($I_{\parallel}$) to perpendicular ($I_{\perp}$) with respect to that of excited light, while the plane of the polarizer is fixed perpendicular to that of incidence:

$$r = (I_{\parallel} - I_{\perp})/(I_{\parallel} + 2I_{\perp}) \qquad (1)$$

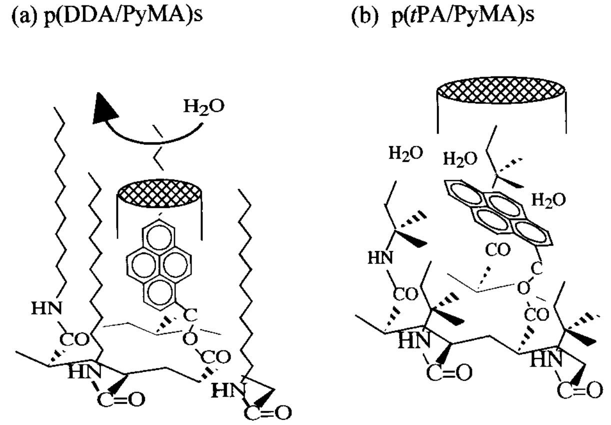

Figure 7. Schematic illustration of the molecular orientation of pyrene in polymer LB films: (a) p(DDA/PyMA)s and (b) p(*t*PA/PyMA)s.

Table 3. Fluorescence Anisotropy *r* for p(DDA/PyMA3) and p(*t*PA/PyMA1)

	r	
	cast film	LB films
p(DDA/PyMA3)	0.20	0.28
p(*t*PA/PyMA1)	0.23	0.29

The results are summarized in Table 3. Comparing the cast and the LB films, the *r* values were found to be larger in the LB films. In general, the cast film is an inflexible matrix, which contains a great deal of free volume. On the other hand, the pyrene residues would be tightly constrained between alkyl side chains in the LB films and more oriented in LB assemblies than in a cast film, accounting for the difference in the *r* values. The dependence of the *r* values on temperature, deposition pressure, and side chain length is a key issue for an understanding of both the molecular environment and the molecular motion in two-dimensional assemblies. These works are now in progress.

The molecular environment of pyrene molecules surrounded by alkyl side chains in LB films is schematically illustrated in Figure 7.

Acknowledgment. The authors acknowledge support by Grant-in Aid for Scientific Research on Priority Areas, “New Polymers and Their Nano-Organized Systems” (No. 277/0910126206), from The Ministry of Education, Science, Sports and Culture of Japan and by the Research for the Future (JSPS-RFTF 97P00302) from The Japan Society for the Promotion of Science.

References and Notes

(1) Ulman, A. *An Introduction to Ultrathin Organic Films: From Langmuir−Blodgett to Self-Assembly*; Academic Press: New York, 1991.
(2) Decher, G.; Hong, J. D.; Schmitt, J. *Thin Solid Films* **1992**, *210/211*, 831.
(3) Kuhn, H.; Möbius, D.; Bücher, H. In *Physical Methods of Chemistry*; Weissberger, A., Rossiter, B. W., Eds.; Wiley: New York, 1972; Vol. 1, Part 3B, p 577.
(4) Bohorquez, M.; Patterson, L. K. *Langmuir* **1990**, *6*, 1739.
(5) Bohorquez, M.; Patterson, L. K. *Langmuir* **1993**, *9*, 2097.
(6) Yamazaki, I.; Tamai, N.; Yamazaki, T. *J. Phys. Chem.* **1987**, *91*, 3572.
(7) Yamazaki, I.; Tamai, N.; Yamazaki, T. *Chem. Phys. Lett.* **1986**, *124*, 326.
(8) Ohmori, S.; Ito, S.; Yamamoto, M. *Macromolecules* **1990**, *23*, 4047.
(9) Tsujii, Y.; Itoh, T.; Fukuda, T.; Miyamoto, T.; Ito, S.; Yamamoto, M. *Langmuir* **1992**, *8*, 936.
(10) Miyashita, T. *Prog. Polym. Sci.* **1993**, *18*, 263.
(11) Miyashita, T.; Mizuta, Y.; Matsuda, M. *Br. Polym. J.* **1990**, *22*, 327.
(12) Taniguchi, T.; Yokoyama, Y.; Miyashita, T. *Macromolecules* **1997**, *30*, 3646.

(13) Feng, F.; Aoki, A.; Miyashita, T. *Chem. Lett.* **1998**, 205.
(14) Ahuja, R. C.; Möbius, D. *Langmuir* **1992**, *8*, 1136.
(15) Yatsue, T.; Miyashita, T. *J. Phys. Chem.* **1995**, *99*, 16047.
(16) The limiting surface area for *t*PA was assumed to be 0.28 nm^2/unit. This was in good agreement with that calculated with the CPK model. See ref 12.
(17) Birks, J. B. *Photophysics of Aromatic Molecules*; Wiley-Interscience: New York, 1970; p 501.
(18) Gullet, J. *Polymer Photophysics and Photochemistry*; Cambridge University Press: Cambridge, 1985; p 141.
(19) Mizuta, Y.; Matsuda, M.; Miyashita, T. *Langmuir* **1993**, *9*, 1110.
(20) Winnik, F. M. *Chem. Rev.* **1993**, *93*, 587.
(21) Nakajima, A. *Bull. Chem. Soc. Jpn.* **1971**, *44*, 3272.
(22) Kalyanasundaram, K.; Thomas, J. K. *J. Am. Chem. Soc.* **1977**, *99*, 2039.
(23) Dong, D. C.; Winnik, M. A. *Can. J. Chem.* **1984**, *62*, 2560.

MA981471X